

# Electrochemistry and Electrogenerated Chemiluminescence Processes of the Components of Aluminum Quinolate/Triarylamine, and Related Organic Light-Emitting Diodes

J. D. Anderson,<sup>†</sup> E. M. McDonald,<sup>‡</sup> P. A. Lee,<sup>†</sup> M. L. Anderson,<sup>†</sup> E. L. Ritchie,<sup>‡</sup> H. K. Hall,<sup>†</sup> T. Hopkins,<sup>†</sup> E. A. Mash,<sup>†</sup> J. Wang,<sup>†</sup> A. Padias,<sup>†</sup> S. Thayumanavan,<sup>§</sup> S. Barlow,<sup>§</sup> S. R. Marder,<sup>†,§</sup> G. E. Jabbour,<sup>||</sup> S. Shaheen,<sup>||</sup> B. Kippelen,<sup>||</sup> N. Peyghambarian,<sup>||</sup> R. M. Wightman,<sup>\*,‡</sup> and N. R. Armstrong<sup>\*,†,||</sup>

Contribution from the Department of Chemistry, University of Arizona, Tucson, Arizona 85721, and Department of Chemistry, University of North Carolina at Chapel Hill, Chapel Hill, North Carolina, Beckman Institute/Jet Propulsion Laboratory/California Institute of Technology, Pasadena, California, and Optical Sciences Center, University of Arizona, Tucson, Arizona 85721

Received March 3, 1998

**Abstract:** Solution electrochemical studies have been conducted of the principle lumophores, dopants, and hole-transport agents of aluminum-quinolate(Alq<sub>3</sub>)-based organic light-emitting diodes (OLEDs) along with the characterization of their electrogenerated chemiluminescence (ECL). In acetonitrile/benzene solvent mixtures, Alq<sub>3</sub> shows single one-electron reduction and oxidation processes, with a separation between the first oxidation and first reduction potentials,  $\Delta E_{\text{electrochemical}} = 3.03$  V, close to the estimates of energy difference between HOMO and LUMO levels obtained from absorbance spectra of thin films of Alq<sub>3</sub>,  $\Delta E_{\text{optical}} = 3.17$  eV. A new sulfonamide derivative of Alq<sub>3</sub>, Al(qs)<sub>3</sub>, showed a positive shift (ca. 0.32 V) in the first reduction potential versus the parent molecule, and resolution of the overall reduction process into three successive, chemically reversible, one-electron reductions. Two successive one-electron oxidations are seen for 4,4'-bis-(*m*-tolylphenylamino)biphenyl (TPD), a hole-transporting material in many bilayer OLEDs, and for TPDF<sub>2</sub>, a fluorinated version of TPD, with TPDF<sub>2</sub> oxidation occurring 0.1 V positive of that for TPD. Electrogenerated chemiluminescence reactions (Alq<sub>3</sub><sup>-•</sup>/TPD<sup>+•</sup> (or TPDF<sub>2</sub><sup>+•</sup>) and Al(qs)<sub>3</sub><sup>-•</sup>/TPD<sup>+•</sup> (or TPDF<sub>2</sub><sup>+•</sup>)) were found to produce emission spectra from Alq<sub>3</sub><sup>\*s</sup> or Al(qs)<sub>3</sub><sup>\*s</sup> states which were nearly identical to those seen from OLEDs based upon these molecules. Emission intensities increased with the increasing potential difference between the relevant redox couples. The diisooamyl derivative of quinacridone (DIQA), a quinacridone dopant for certain Alq<sub>3</sub>-based OLEDs, undergoes two successive one-electron reductions and two successive one-electron oxidations. The ECL reactions DIQA<sup>-•</sup>/DIQA<sup>+•</sup>, DIQA<sup>+•</sup>/Alq<sub>3</sub><sup>-•</sup>, DIQA<sup>+•</sup>/Al(qs)<sub>3</sub><sup>-•</sup>, DIQA<sup>-•</sup>/TPD<sup>+•</sup> and DIQA<sup>-•</sup>/TPDF<sub>2</sub><sup>+•</sup> all produce the same singlet emissive state, DIQA<sup>\*s</sup>, and the same emission spectral response seen in quinacridone and DIQA-doped OLEDs.

## Introduction

There is substantial interest in the development of new light sources based upon formation of emissive states in thin films of organic dyes, through direct injection of electrical charge into single layer or multilayer thin films (organic light-emitting diodes, OLEDs, or organic electroemissive devices, OEDs).<sup>1–3</sup> The interest in this type of electrically pumped luminescence

can be traced back several decades to observations of light emission in thin films of single-crystal molecular materials such as anthracene<sup>1c</sup> and to studies of several electrochemically driven light emission processes at molecular crystal electrodes<sup>2</sup>. Two different classes of materials have emerged recently based upon ultrathin films of (a) extended conjugation polymers exhibiting strong luminescence (e.g., derivatives of polyparaphenylene-vinylene, PPV, and related luminescent polymers)<sup>3</sup> and (b) vacuum-deposited small molecule systems including tris(8-quinolinolato-N<sub>1</sub>O<sub>8</sub>)aluminum (Alq<sub>3</sub>, **1**) (Scheme 1), and several other vacuum-compatible luminescent dyes.<sup>4</sup>

The vacuum-deposited small molecule OLEDs are also often doped with low concentrations of other dyes such as quinacridones (e.g., **5** and **6**) with longer wavelength emissions, which

\* To whom correspondence should be addressed. E-mail: nra@u.arizona.edu.

<sup>†</sup> Department of Chemistry, University of Arizona.

<sup>‡</sup> University of North Carolina at Chapel Hill.

<sup>§</sup> Beckman Institute/Jet Propulsion Laboratory/California Institute of Technology.

<sup>||</sup> Optical Sciences Center, University of Arizona.

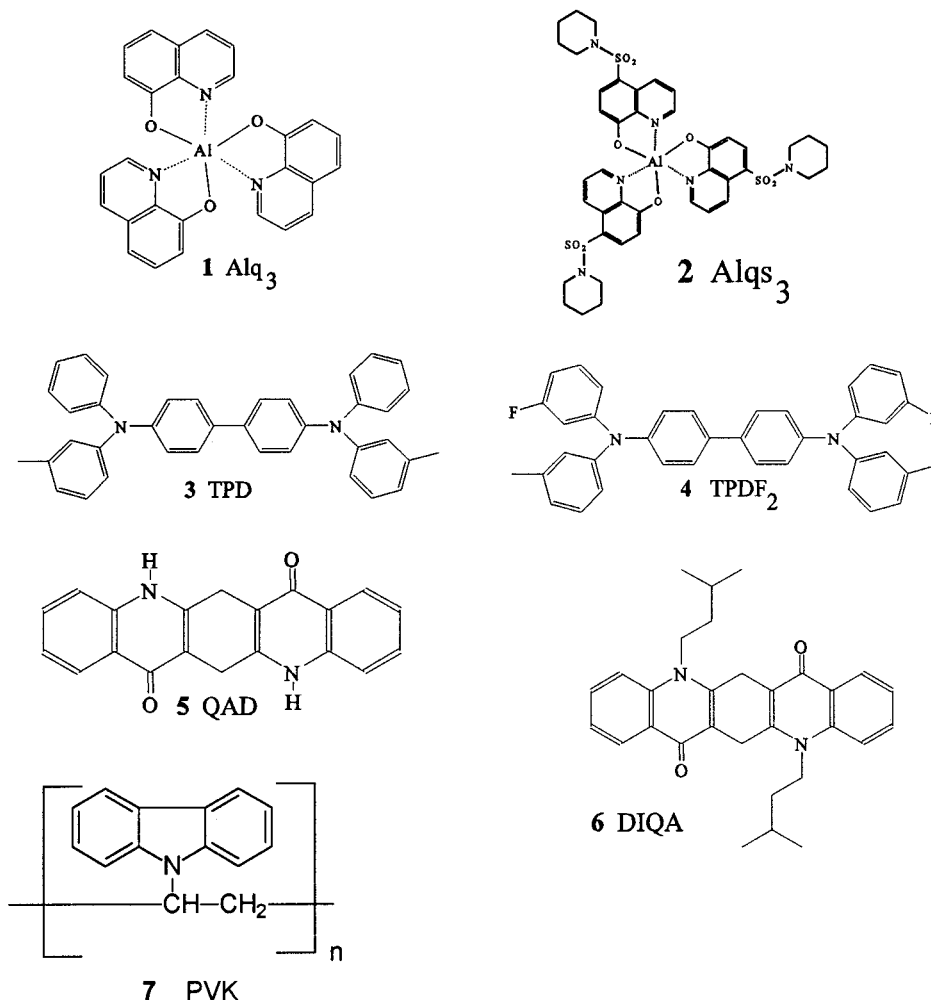
(1) (a) Rothberg, L. J.; Lovinger, A. J. *J. Mater. Res.* **1996**, *11*, 3174 and references therein. (b) Sheats, J. R.; Antoniadis, H.; Hueschen, M.; Leonard, W.; Miller, J.; Moon, R.; Roitman, D. *Science* **1996**, *273*, 884. (c) Dresner, J. *RCA Rev.* **1969**, *30*, 322.

(2) Mehl, W.; Hale, J. M. *Advances in Electrochemistry and Electrochemical Engineering*; Delahay, P., Ed.; Wiley-Interscience: New York, 1967; Vol. 6, p 399 and references therein.

(3) Friend, R. H.; Greenham, N. C. In *Handbook of Conducting Polymers*, 2nd ed.; Skotheim, T. A., Elsenbaumer, R. L., Reynolds, J. R., Eds.; Marcel Dekker: New York, 1998; pp 823–846 and references therein.

(4) (a) Tang, C. W.; VanSlyke, S. A. *Appl. Phys. Lett.* **1987**, *51*, 913. (b) Tang, C. W.; VanSlyke, S. A.; Chen, C. H. *J. Appl. Phys.* **1989**, *65*, 3610. (c) Tang, C. W. *Society for Information Display International Symposium Digest of Technical Papers*; SID: Santa Ana, CA, 1996; p 181. (d) Shi, J.; Tang, C. W. *Appl. Phys. Lett.* **1997**, *70*, 1665. (e) Tang, C. W.; VanSlyke, S. A.; Chen, C. H. *J. Appl. Phys.* **1989**, *65*, 3610. (f) VanSlyke, S. A.; Chen, C. H.; Tang, C. W. *Appl. Phys. Lett.* **1996**, *69*, 2160. (g) Jabbour, G. E.; Kawabe, Y.; Shaheen, S. E.; Wang, J. F.; Morrell, M. M.; Kippelen, B.; Peyghambarian, N. *Appl. Phys. Lett.* **1997**, *71*, 1762.

Scheme 1



allow for enhancement of the electroluminescent response and color tuning.<sup>3,4</sup> Thin film mixtures of electroemissive, ion-conducting polymers and supporting electrolytes have also been developed where light generation occurs through electrochemically generated luminescence processes.<sup>5</sup>

In vacuum-deposited devices, 100–200-nm thickness luminescent dye films, such as Alq<sub>3</sub> (LUM in Figure 1a, left panel), are sandwiched between injecting electrodes of different work functions (indium–tin oxide, ITO, as the anode, and low work function metals, e.g., Al, Ag/Mg, Ca, or Li and lithium alloys, as the cathodes)(Figure 1a, left panel). Charge transporting organic layers (triarylamines such as 4,4'-bis(*m*-tolylphenylamino)biphenyl (TPD, **3**), and several related molecules,<sup>4</sup> or poly(*N*-vinylcarbazole) (PVK, **7**)), are interposed between these contacting electrodes and the lumophore layer (HTL in Figure 1a, left panel). Resultant multilayer thin film assemblies possess electrical conductivities less than 10<sup>-10</sup> Ω<sup>-1</sup> cm<sup>-1</sup> and experience electric field gradients up to 10<sup>6</sup> volts per cm during operation.<sup>4</sup> Conduction occurs through the hopping of charges (polarons) between adjacent molecules. Cation radicals are the likely “hole” in these triarylamine or PVK layers, while radical anions are presumed to be the form of the injected electron in the lumophore layer.<sup>6–8</sup>

The energy barrier to hole injection from the triarylamine layer into the lumophore layer has been estimated recently to be from ca. 0.3 to 0.4 eV.<sup>9</sup> The hole-transport layer also provides a significant energy barrier (≥0.3 eV) against electron injection from the lumophore layer toward the anode, and generally exhibits low electron mobilities. The lumophore layer typically shows electron mobilities which are ca. 2 orders of magnitude lower than hole-transport mobilities in the triarylamine layers, and hole mobilities which are 2–4 orders of magnitude lower than hole mobilities in the triarylamine layers.<sup>6–8</sup> These disparities in mobilities, and the energy barriers to charge injection at the interface between the two organic thin films, create the rectifying current–voltage response of the

(5) (a) Richter, M. M.; Fan, F.-R. F.; Klavetter, F.; Heeger, A. J.; Bard, A. J. *Chem. Phys. Lett.* **1994**, *226*, 115. (b) Dick, D. J.; Heeger, A. J.; Pei, Q. *Adv. Mater.* **1996**, *8*, 985. (c) Pei, Q.; Yang, Y.; Heeger, A. J. *J. Am. Chem. Soc.* **1996**, *118*, 3922. (d) Mannes, K. M.; Terrill, R. H.; Meyer, T. J.; Murray, R. M.; Wightman, R. M. *J. Am. Chem. Soc.* **1996**, *118*, 10609. (e) Gao, J.; Yu, G.; Heeger, A. J. *Appl. Phys. Lett.* **1997**, *71*, 1293.

(6) (a) Redecker, M.; Bäessler, H. *Appl. Phys. Lett.* **1996**, *69*, 70. (b) Redecker, M.; Bäessler, H.; Hörhold, H. H. *J. Phys. Chem.* **1997**, *101*, 7398. (c) Pommerhene, J.; Vestweber, H.; Guss, W.; Mahrt, R. F.; Bäessler, H.; Porsch, M.; Daub, J. *Adv. Mater.* **1995**, *7*, 551.

(7) (a) Borsenberger, P. M.; Weiss, D. S. *Organic Photoreceptors for Imaging Systems*; Marcel Dekker: New York, 1993; pp 181–272 and references therein. (b) Lin, L.-B.; Jenekhe, S. A.; Young, R. H.; Borsenberger, P. M. *Appl. Phys. Lett.* **1997**, *70*, 2052. (c) Kepler, R. G.; Beeson, P. M.; Jacobs, S. J.; Anderson, R. A.; Sinclair, M. B.; Valencia, V. S.; Cahill, P. A. *Appl. Phys. Lett.* **1995**, *66*, 3618.

(8) (a) Facci, J. S.; Abkowitz, M. A.; Limburg, W. W.; Renfer, D. S.; Yanus, J. F. *Mol. Cryst. Liq. Cryst.* **1991**, *194*, 55. (b) Facci, J. S.; Abkowitz, M. A.; Limburg, W. W.; Knier, F.; Yanus, J. F.; Renfer, D. S. *J. Phys. Chem.* **1991**, *95*, 7908. (c) Abkowitz, M. A.; Facci, J. S.; Limburg, W. W.; Yanus, J. F. *Phys. Rev. B* **1992**, *46*, 7908.

(9) (a) Schlaf, R.; Lee, P. A.; Nebesny, K. W.; Parkinson, B. A.; Armstrong, N. R. *Appl. Phys. Lett.* **1998**, *73*, 1026. (b) Rajagopal, A.; Wu, C. I.; Kahn, A. J. *Appl. Phys.* **1998**, *83*, 2649. (c) Anderson, M., Ph.D. Dissertation, University of Arizona, 1997.

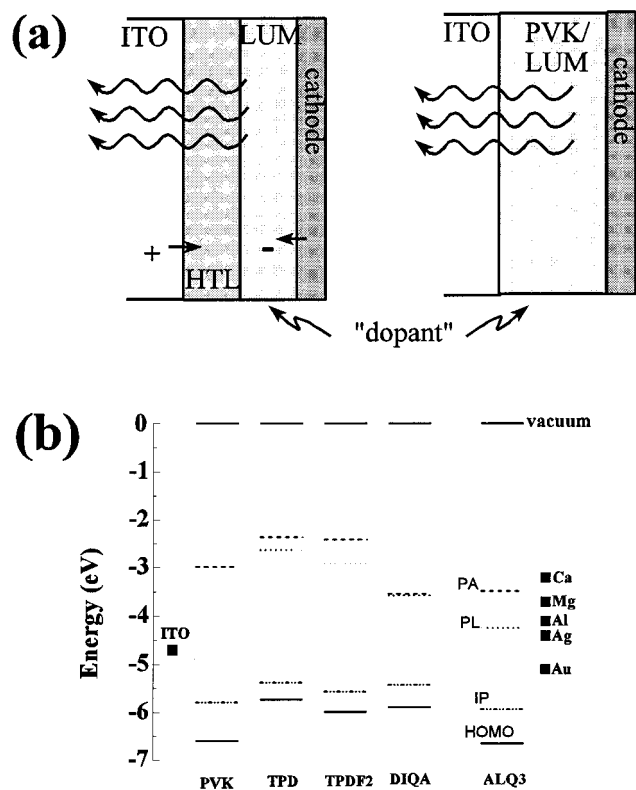


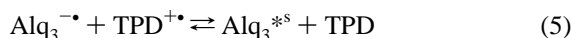
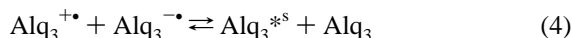
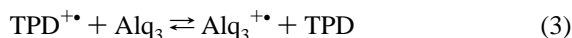
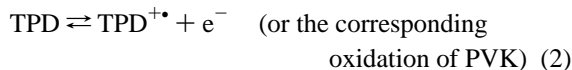
**Figure 1.** (a) Schematic of two types of organic light-emitting diodes involving molecular emitters such as Alq<sub>3</sub>; the left panel shows the configuration of an OLED using an ITO/hole-transport layer (like TPD)/lumophore (like Alq<sub>3</sub>)/cathode; the right panel shows a single layer device, based upon the lumophore dissolved into a hole-transporting polymer such as PVK. (b) Ionization levels (IP) and HOMOs (relative to vacuum) estimated from UPS characterization of thin films of several luminescent and charge-transporting molecules (see text). Also shown are the energies for absorption (PA) and luminescence (PL) measured from the HOMO energy, along with the anticipated positions of the Fermi energies for the contacting electrodes, based upon established work functions for these materials.

device.<sup>4</sup> The HTL/LUM interface region provides a location where the radical states of these molecules can collect and recombine, avoiding their recombination close to the cathode, where quenching of the resultant luminescence may occur.<sup>4</sup>

Single layer OLEDs can also be created from hole-transporting polymers, such as PVK, into which *both* lumophores and dopants have been added (Figure 1a, right panel), where there is no identifiable heterojunction between the hole-transporting host and the lumophore.<sup>1,10</sup> The efficiencies of these devices are more difficult to optimize than those of the vacuum deposited bilayer devices; however, wide variations in lumophore concentration and the ratio of lumophore-to-dopant concentrations are easily obtained.<sup>9,10</sup> Tris(5-piperidinylsulfonamide-8-quinolinolato-N<sub>1</sub>O<sub>8</sub>)aluminum (Al(qs)<sub>3</sub>, **2**), a new derivative of Alq<sub>3</sub>, is of interest for use in these single layer devices.<sup>11</sup> The sulfonamide substituent increases the solubility of the metal quinolate in common solvents and polymers and has the effect of blue-shifting both the absorbance and luminescence maxima.

For both types of OLEDs, questions remain whether hole injection to the lumophore (oxidation of **1** or **2**) is necessary to

carry out the annihilation reactions which create the emissive state of that molecule (eqs 1–4) or whether it would be sufficient for the hole (cation radical) state of the hole-transport material (PVK<sup>•+</sup> or TPD<sup>•+</sup>) to annihilate with the electron-rich state (radical anion) of the lumophore (eqs 1 and 2, followed by 5), to create this emissive state.



Equation 5 is simply a version of well-established “cross reactions” which have been shown to occur in solution between lumophores such as diphenylanthracene (DPA), rubrene, and various oxidizable amines.<sup>12,13</sup> The energy released in such a cross reaction is not as high as for the direct annihilation of both radical states of the lumophore but may be enough to produce the singlet emissive state of the lumophore directly (singlet pathway, energy sufficient) or may be large enough to produce this singlet state through the formation of triplet states of the lumophore (triplet pathway, energy insufficient), followed by triplet–triplet annihilation reactions.<sup>12,13</sup> Voltammetric and ECL studies presented here show that the reactions represented in eq 5, for both Alq<sub>3</sub> and Al(qs)<sub>3</sub>, lead to singlet emissive states for the metal quinolate. Increasing the driving force for the cross reaction indicated in eq 5, through the use of the fluorinated TPD derivative, **4**, with a higher first oxidation potential, increases the ECL efficiency.

Such a cross reaction in the condensed phase would represent an alternative (parallel) pathway to the formation of the emissive state of Alq<sub>3</sub>, which would not require direct injection of a hole (oxidation of Alq<sub>3</sub>). Versions of this reaction would provide for the formation of the emissive state of the lumophore at the HTL/LUM interface for bilayer OLEDs or throughout the entire film in single layer OLEDs. This pathway may also be important in OLEDs based on bilayers of luminescent polymers, such as PPV and related cyano-PPV derivatives, where one polymer layer has been optimized for hole transport, the other layer for electron transport, and the interface between these layers exhibits the same type of rectifying electrical characteristics seen for the Alq<sub>3</sub>/TPD OLEDs.<sup>3</sup>

Quinacridone, **5**, and its bis(*N*-methyl) derivative are effective dopants for aluminum quinolate OLEDs.<sup>4d,e,10</sup> The parent compound is strongly aggregated in concentrated solutions and in the solid state through hydrogen bonding interactions between adjacent molecules along with van der Waals interactions.<sup>14</sup> For

(12) (a) Faulkner, L. R.; Bard, A. J. In *Electroanalytical Chemistry*; Bard, A. J., Ed.; Marcell Dekker: New York, 1977; Vol. 10, p 1. (b) Debad, J. D.; Morris, J. C.; Lynch, V.; Magnus, P.; Bard, A. J. *J. Am. Chem. Soc.* **1996**, *118*, 2374.

(13) (a) Maness, K. M.; Wightman, R. M. *J. Electroanal. Chem.* **1995**, *396*, 85. (b) Collinson, M. M.; Wightman, R. M. *Anal. Chem.* **1993**, *65*, 2576. (c) Collinson, M. M.; Wightman, R. M.; Pastore, P. *J. Phys. Chem.* **1994**, *98*, 11942. (d) Maness, K. M.; Bartelt, J. E.; Wightman, R. M. *J. Phys. Chem.* **1994**, *98*, 3993. (e) Ritchie, E. L.; Pastore, P.; Wightman, R. M. *J. Am. Chem. Soc.* **1997**, *119*, 11920. (f) Ritchie, E., M.S. Thesis, University of North Carolina, 1997.

(14) (a) Kalowski, J.; Stampor, W.; DiMarco, P.; Fattori, V. *Chem. Phys.* **1994**, *182*, 341. (b) Schilling, B.; Back, A.; Armstrong, N. R., manuscript in preparation.

(10) Shaheen, S. E.; Kawabe, Y.; Wang, J. F.; Anderson, J. D.; Morrell, M. M.; Jabbour, G. E.; Kippelen, E. A.; Mash, E. A.; Armstrong, N. R.; Peyghambarian, N. *J. Phys. Chem.*, submitted.

(11) Hopkins, T. A.; Meerholz, K.; Shaheen, S.; Anderson, M. L.; Schmidt, A.; Kippelen, B.; Padias, A. B.; Hall, H. K., Jr.; Peyghambarian, N.; Armstrong, N. R. *Chem. Mater.* **1996**, *8*, 344.

the new isoamyl derivative (DIQA, **6**) and methyl derivatives,<sup>4d</sup> these interactions are significantly weakened.<sup>10,14b</sup> UPS studies of the frontier orbitals of both QAD and DIQA show that they may act as an electron acceptor from Alq<sub>3</sub><sup>-•</sup> or an electron donor to Alq<sub>3</sub><sup>+•</sup> in the condensed phase.<sup>10</sup> In an homogeneous Alq<sub>3</sub>/PVK OLED, systematic increases in DIQA concentration quench the Alq<sub>3</sub> electroluminescence at a greater rate than the Alq<sub>3</sub> photoluminescence.<sup>10</sup>

The solution electrochemical properties of DIQA confirm that it may act as an electron acceptor from Alq<sub>3</sub><sup>-•</sup>, as a weak electron donor to Alq<sub>3</sub><sup>+•</sup>, and as a poor donor to the cation radicals of TPD, TPDF<sub>2</sub>, and PVK. ECL reactions between the cation and anion radical states of DIQA (eq 6) and between



the radical states of DIQA and those of either Alq<sub>3</sub> or TPD (eqs 7 and 8) are shown to form the same emissive state in solution as found in DIQA-doped Alq<sub>3</sub> devices:

### Experimental Section

All chemicals were obtained from Aldrich without further purification unless noted herein. Nitrogen degassed anhydrous acetonitrile and benzene from Fischer were passed through an activated basic alumina column prior to use. Ferrocene was recrystallized from ethanol. Tetrabutylammonium hexafluorophosphate (TBAH) was recrystallized twice from anhydrous ethanol and dried in a vacuum oven at 40 °C for 24 h. 4,4'-Bis(*m*-tolylphenylamino)biphenyl (TPD, **3**) was further purified by gradient sublimation. Tris(8-quinolinolato-N<sub>1</sub>O<sub>8</sub>)aluminum (Alq<sub>3</sub>, **1**) was obtained from Aldrich and purified by gradient sublimation. Poly(*N*-vinylcarbazole) (PVK, **7**) was obtained from Aldrich and purified twice by precipitation from a dichloromethane solution with methanol. Preparations of tris(5-periperidynylsulfonamide-8-quinolinolato-N<sub>1</sub>O<sub>8</sub>)aluminum (Alq<sub>3</sub>, **2**) and 4,4'-bis(*m*-fluorophenyl-*m*-tolylamino)biphenyl (TPDF<sub>2</sub>, **4**) have been recently published.<sup>11,15</sup> The full description of the synthesis of *N,N'*-diisoamylquinacridone (DIQA, **6**) is presented elsewhere.<sup>10</sup>

Ultraviolet photoelectron spectroscopy (UPS) of the pure thin film materials was carried out using a 21.8 eV He (I) source in a VG ESCALAB MKII photoelectron spectrometer, according to procedures developed previously for a wide range of molecular systems.<sup>9,16</sup> The sample was biased with an external power supply during data acquisition, to allow for the measurement of the low kinetic energy cutoff region, which helps to define the binding energy scale for these spectra with respect to vacuum. Gas-phase UPS spectra (also using a He (I) source) were obtained in a modified spectrometer with appropriate sublimation sources so as to obtain a sufficient fluency of material to allow for adequate signal collection.<sup>17</sup>

Estimates of LUMO positions and electron affinities (EA) were made using the absorbance and fluorescence spectra of these materials as thin films. UV-visible absorption spectra were recorded on thin films on transparent substrates with the same surface coverages as those used for the UPS measurements, using a Hitachi U-2000 spectrophotometer. Luminescence spectra of these same films were recorded with an ISA Fluorolog spectrofluorimeter.

Normal cyclic voltammograms were taken with an EG&G Instruments 283 potentiostat, using a freshly polished Pt disk electrode with a geometric area of 0.32 cm<sup>2</sup>. Millimolar concentrations of the molecules of interest were dissolved in a nitrogen-degassed mixture of 1:1 benzene/

acetonitrile (MeCN) solvent mixture, which was made with 0.1 M in tetrabutylammonium hexafluorophosphate (TBAHFP) as the supporting electrolyte. The electrochemical cell was degassed with UHP nitrogen prior to analysis. Potential sweep rates ranged from 100 to 1000 mV/s. The potential of the Pt electrode was controlled versus a Ag/AgCl pseudoreference electrode, and at the end of each set of voltammetric experiments, ferrocene was added to the solution (to create a millimolar solution concentration) and the oxidation/reduction of this molecule characterized, so as to provide a Fc/Fc<sup>+</sup> reference potential for each voltammetric experiment.<sup>18</sup> The number of electrons transferred in the reduction and oxidation of compounds **1–6** were estimated from the peak currents in these voltammograms, comparing these peak currents with those seen for the redox processes of comparable concentrations of either diphenylanthracene (DPA) or ferrocene in the same solvent.<sup>19</sup> We assume that the diffusion coefficients for DPA and these compounds are comparable (within 1/2 an order of magnitude).

ECL reactions were characterized with a high-speed microelectrode protocol using a previously described apparatus.<sup>13</sup> The electrochemical cell was configured in a flow-cell geometry. A gold band electrode with a 3-μm thickness, ca. 0.5 cm in length, was flush-mounted in an epoxy mold containing a silver band pseudoreference electrode and placed in the flow cell directly opposite a window where a photomultiplier detector was positioned. Potential steps were applied to the working electrode with a frequency of 1 kHz. The working electrode potential in these experiments was controlled by a Hewlett-Packard function generator (HP33120A) connected to the potentiostat. To measure the spectral response of the ECL process, an optical fiber bundle pickup (Oriel model 77538) routed the ECL emission to a JY Optical Systems (H-20) monochromator, with a 2-nm band-pass, followed by the same PMT detector. Light was detected in both cases with a Hamamatsu R5600P photomultiplier tube, operated at -800 V. The PMT output was routed to an EG&G Ortec VT120A preamplifier, connected to a multichannel scaler (EG&G Ortec MCS T-914) with a discriminator level set at -300 mV. The working electrode was connected to a fast current-to-voltage converter with gain settings of 5 × 10<sup>5</sup> or 1.25 × 10<sup>7</sup> V/A. A digital oscilloscope (Lecroy 9450) was used to monitor the applied potential, current, and ECL responses.

For each ECL experiment, the solvent mixture (acetonitrile/toluene, 50/50 vol %) was delivered by the pump to the electrochemical cell at a flow rate of 200 μL/in. A loop injector was used to introduce reagents to the cell from a reservoir of acetonitrile, 0.1 M in TBAH, previously degassed with nitrogen. During the ECL experiments, the potential of the working electrode was cycled between potential limits established to lie 100 to 200 mV beyond the potentials needed to reduce or oxidize the target molecules at diffusion controlled rates.<sup>13</sup> ECL efficiencies were estimated by examining the emission achieved from a 10<sup>-3</sup> M diphenylanthracene (DPA) solution, in the same solvent, which has been previously shown to have a quantum efficiency of 6.3%.<sup>13d</sup> The wavelength dependence of the PMT efficiency was then corrected to allow for correlation of the ECL efficiency of DPA with the efficiency observed in these experiments at longer wavelengths. PMT counts were binned at 100 kHz for 2 complete cycles of the square wave and the sum of 50 or 1000 total cycles was then summed (0.1 or 2.0 s total data acquisition time). ECL spectra were obtained by setting the MCS dwell time equal to the speed of the wavelength scan controller (200 or 1000 nm per minute), depending upon the electrochemical stability of the system used. ECL emission spectra were also corrected for the wavelength dependence of PMT sensitivity.

### Results and Discussion

#### Frontier Orbital Energies and Basic Electrochemical Processes

Use of solution electrochemical processes to describe electron-transfer reactions in the condensed phase is predicated upon

(15) Thayumanavan, S.; Barlow, S.; Marder, S. *Chem. Mater.* **1997**, *8*, 490.

(16) Schmidt, A.; Anderson, M. L.; Armstrong, N. R. *J. Appl. Phys.* **1995**, *78*, 5619.

(17) Ray, C. D.; Nebesny, K. W.; Lamb, L. D.; Huffman, D. R.; Lichtenburger, D. L. *Chem. Phys. Lett.* **1991**, *176*, 203.

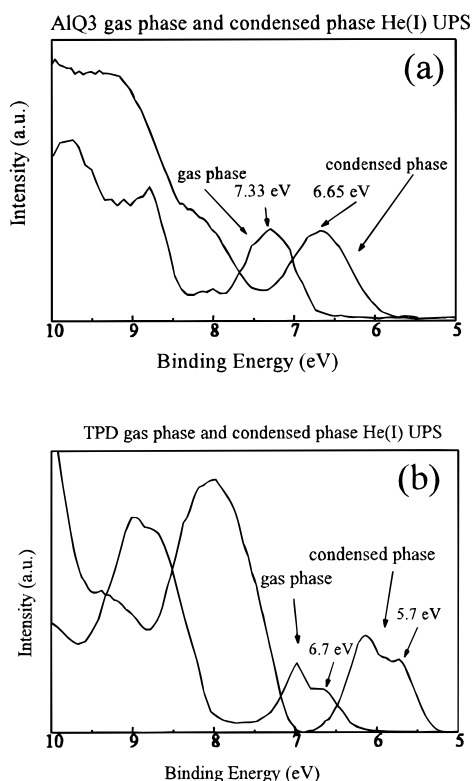
(18) Sawyer, D. T.; Sobkowiak, A.; Roberts, J. L. *Electrochemistry for Chemists*, 2nd ed.; John Wiley and Sons: New York, 1995; pp 203–204 and references therein.

(19) Bard, A. J.; Faulkner, L. R. *Electrochemical Methods*; John Wiley and Sons: New York, 1980; pp 215–242 and references therein.

**Table 1.** Estimates of HOMO, IP, and LUMO Levels Using Thin Film UPS Data and Solution and Thin Film Absorbance/Luminescence Data for the Two Forms of Aluminum Quinolate Described Here, the Three Hole-Transport Materials, and the Dopant Quinacridone Derivative (see text)

compound	HOMO [eV] ± 0.15 eV	IP [eV] ± 0.15 eV	lowest energy PA <sub>max</sub> [eV]	(0-0 phonon) PL <sub>max</sub> [eV]	PA state [eV] ± 0.15 eV	PL state [eV] ± 0.15 eV	V <sub>red</sub> vs Fc/Fc <sup>+</sup>	V <sub>ox</sub> vs Fc/Fc <sup>+</sup>
Alq <sub>3</sub>	6.65	5.93	3.17	2.40	3.48	4.25	-2.30	0.73
Al(qs) <sub>3</sub>	6.50 (± 0.25 eV)	5.66 (± 0.25 eV)	3.26	2.47	3.24	4.03	-1.98	1.04
DIQA	5.89	5.42	2.35	2.32	3.54	3.57	-1.84	0.70
TPD	5.73	5.38	3.37	3.10	2.36	2.63		0.35
TPDF <sub>2</sub>	5.99	5.56	3.58	3.08	2.41	2.91		0.45
PVK	6.60	5.79	3.62		2.98			0.56 <sup>a</sup>

<sup>a</sup> Estimated from dilute solutions of PVK oligomers and from electropolymerized PVK on a gold electrode.

**Figure 2.** Gas phase and condensed phase UPS spectra for Alq<sub>3</sub> and TPD, corrected for spectrometer work function differences.

the assumption that the differences in ionization potential and electron affinity of these molecules in solution are equal to or smaller than those same energy differences in the condensed phase. For example, if the driving force for eq 5 is found sufficient to create the singlet emissive state of Alq<sub>3</sub> in solution, we argue below that this driving force will be the same or larger in the condensed phase, for Alq<sub>3</sub> and for other weakly interacting molecular systems which might be used in OLEDs.

Figure 2 shows both the gas phase and condensed phase UPS data for the Alq<sub>3</sub> and TPD systems. Table 1 and Figure 1b summarize the frontier orbital positions obtained from UPS of vapor-deposited pure thin films of each of the components of this study on Au and Ag substrates.<sup>9c,16</sup> We also show the anticipated Fermi energies for the contacting electrodes, the ITO anode, and several of the cathodes most often used in these devices. UPS studies provide an estimate of the ionization potential (IP) and the median energy of the highest occupied molecular orbital (HOMO) for those aromatic molecular systems where the HOMO is well-resolved in energy from the next highest molecular orbital and composed primarily of C(2p<sub>z</sub>) orbitals.<sup>9,16</sup> The fwhm of the gas phase spectra are smaller by only ca. 40% relative to the condensed phase spectra, indicating

comparable lifetimes of the core hole state produced in the photoelectron spectroscopic event, consistent with the weak intermolecular interactions (no significant aggregation) and relaxation effects in the solid state for these materials.<sup>20</sup> The absolute differences between the gas phase and the condensed phase HOMO binding energies are ca. 0.8 eV for Alq<sub>3</sub> and ca. 1.0 eV for TPD, owing to differences in stabilization of the core hole state following the photoionization process.<sup>20</sup> The differences in median HOMO energy for pure thin films of TPD vs Alq<sub>3</sub> is  $\Delta\text{HOMO} = \text{ca. } 0.8 \text{ eV}$ . Recent experiments to characterize  $\Delta\text{HOMO}$  when the two materials are in contact with each other, as TPD/Alq<sub>3</sub> or Alq<sub>3</sub>/TPD bilayers, show that  $\Delta\text{HOMO}$  is reduced to ca. 0.4 eV,<sup>9a</sup> a value which is also close to that observed for the heterointerface formed between Alq<sub>3</sub> and a closely related derivative of TPD.<sup>9b</sup>

UPS studies of Al(qs)<sub>3</sub> were complicated by our inability to vaporize this molecule, necessitating its study as thin films deposited from hexane solutions onto graphite substrates.<sup>9c</sup> The photoemission peak positions determined for this molecule were within 0.2 eV of those determined for Alq<sub>3</sub>, with  $\pm 0.25 \text{ eV}$  uncertainty in their position. Electrochemical results discussed below suggest that these values significantly underestimate the true HOMO and IP for this molecule.

The LUMO positions for these molecular systems, estimated using the energy maxima of the thin film absorbance bands (PA state) for each material, are also listed in Table 1. It is also possible to use the HOMO position as a reference and the difference between first oxidation and first reduction potentials in solution to make an estimate of LUMO position. The orbital into which an electron is injected during reduction in solution or in the solid-state device, however, may not be the same one occupied during spectroscopic excitation. The energy of a reduced or oxidized molecule is typically different by ca. 0.1 eV or greater from the "conduction band" or "valence band" states for the molecular solid.<sup>21</sup> Exact measurements of the HOMO/LUMO energy gap,  $\Delta E$ , in the condensed phase await measurements of the electron affinity of both Alq<sub>3</sub> and TPD thin films, as have been recently reported for C<sub>60</sub> and the perylenetetracarboxydianhydride dye, PTCDA.<sup>21</sup> Our estimates of this energy gap, based upon spectroscopic and electrochemical measurements (below) and combined with the UPS data, nevertheless agreed within 0.2 eV for Alq<sub>3</sub> where both oxidation and reduction processes could be observed in solution (see below,  $\Delta E_{\text{electrochemical}} = 3.03 \text{ eV}$ ,  $\Delta E_{\text{optical}} = 3.17 \text{ eV}$ ). A comparable level of agreement was seen for DIQA (Table 1).

(20) (a) Brundle, C. R.; Baker, A. D. In *Electron Spectroscopy, Theory, Techniques and Applications*; Brundle, C. R.; Baker, A. D., Eds.; Academic Press: New York, 1977, pp 45-49. (b) Martin, R. L.; Shirley, D. A. In *Electron Spectroscopy, Theory, Techniques and Applications*; Brundle, C. R.; Baker, A. D., Eds.; Academic Press: New York, 1977; pp 86-117.

(21) (a) Rajagopal, A.; Kahn, A. *Adv. Mater.* **1998**, *10*, 140. (b) Weaver, J. H. *J. Phys. Chem. Solids* **1992**, *53*, 1433.

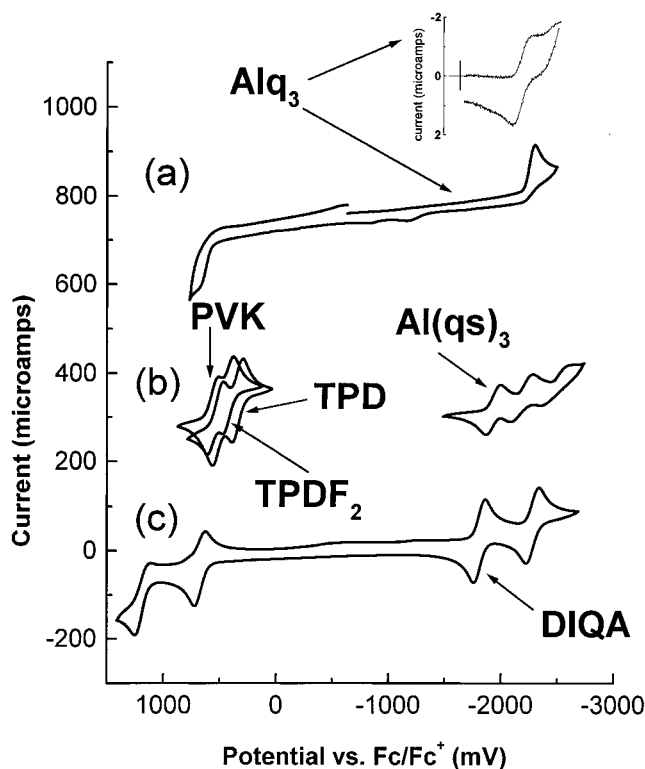


**Figure 3.** Cyclic voltammograms for (a)  $\text{Alq}_3$ , both oxidation and reduction processes shown in the main voltammogram, an inset is shown above this main voltammogram, showing the cyclic voltammetric behavior (charging current background corrected) for this compound at the gold microband electrode used for the ECL experiments (see text), at a sweep rate of 2000 V/s, showing the chemical reversibility of the reduction process at this sweep rate; (b)  $\text{Al}(\text{qs})_3$  (only reductions shown) and TPD and  $\text{TPDF}_2$  (oxidations shown) (the position of the oxidation peak potential for an oligomer solution of PVK is also indicated); and (c) DIQA. Solution concentrations were ca.  $10^{-3}$  M, sweep rates were 100 mV/s. The scans in (b) and (c) have been offset by 300 and 700  $\mu\text{A}$ , respectively, to improve clarity of presentation.

Figure 3 and Table 1 summarize the voltammetric behavior of  $10^{-3}$  M solutions of  $\text{Alq}_3$  **1**, its sulfonamide derivative **2**, TPD **3**, its difluoro derivative **4**, the quinacridone derivative, DIQA **6**, and ca. 0.1 mM solutions of oligomeric PVK **7**.<sup>9c</sup> For all of the compounds shown here, we estimated the number of electrons transferred in each voltammetric process by comparing the peak current at a fixed sweep rate with that seen for compounds where the number of electrons transferred in the voltammetric process was known. The oxidation and reduction processes for diphenylanthracene, ferrocene, and the TPD derivatives all gave comparable peak currents to the new compounds discussed in this paper, after corrections for differences in the diffusion coefficient which arise because of differences in molecular size.<sup>19</sup>

$\text{Alq}_3$  undergoes a single reduction process and a single oxidation process within the solvent window, with peak potentials of ca.  $-2.30$  V and  $+0.73$  V vs  $\text{Fc}/\text{Fc}^+$ . Both processes are chemically irreversible on the time scale of the experiment shown in Figure 3 (sweep rate of 100 mV/s). Voltammetric experiments at sweep rates of 2000 V/s,<sup>9d</sup> however, showed complete chemical reversibility of the one-electron reduction process, while intermediate sweep rate experiments allowed us to estimate the half-life of  $\text{Alq}_3^{\cdot-}$  as ca. 0.05 s.<sup>19</sup> Peak potentials were used to estimate the differences in  $E^{\circ'}$  values for the reduction and oxidation processes of  $\text{Alq}_3$  and the other compounds discussed below, recognizing that the peak potentials for  $\text{Alq}_3$  redox processes

may deviate from the true  $E^{\circ'}$  values by up to 0.05 V, due to the sweep rate dependence of the positions of these voltammetric peaks, due to the chemical instability of  $\text{Alq}_3^{\cdot-}$  and  $\text{Alq}_3^{\cdot+}$ .<sup>19</sup>

In the case of the sulfonamide derivative **2**, the first reduction process is shifted positively relative to that seen for the parent compound to  $-1.98$  V vs  $\text{Fc}/\text{Fc}^+$ . Three successive chemically reversible reduction processes are seen, with a current magnitude at this concentration consistent with the reduction of each of the quinolate groups by one electron. The spacing between the voltammetric waves suggests that these quinolate groups experience intramolecular interactions such that the reduction of the first quinolate group on the molecule affects the reduction potential of the successive electron-transfer events.<sup>22</sup> The presence of these three successive voltammetric processes implies that a similar reduction series ought to be seen for the parent compound **1** and that only the first reduction is observable within the solvent window. The enhanced stability of the radical anion form of  $\text{Al}(\text{qs})_3$  is evident from the peak current ratio for those voltammograms, showing a half-life of at least 20 s. The oxidation process for **2** was much less reversible on the time scale of these voltammetric experiments, regardless of solvent composition, and further complicated by adsorption to the electrode surface.

The oxidation of TPD and  $\text{TPDF}_2$ , **3** and **4**, respectively proceeds by two successive one-electron oxidations, as earlier shown by Facci and co-workers for a linked pair of triarylamines weakly interacting through the biphenyl linkage.<sup>8</sup> The addition of the fluorine substituents increases the first oxidation potential of the triarylamine moiety by ca. 0.1 V. The oxidation products for TPDs are stable on the voltammetric time scale, with half-lives of at least several minutes in the solvents explored here. No reduction processes were observable for these molecules within the solvent window, as expected from the UPS/spectroscopic estimates of electron affinities.<sup>9,16</sup> Several additional derivatives of the TPD series have been created,<sup>15</sup> where the substituents shift the first oxidation potential positively or negatively and affect the voltammetric resolution of the two successive oxidation events. These substitution patterns also greatly affect the stabilities of the cation radical states. The details of these studies will be reported shortly.

The oxidation of solvent-soluble PVK oligomers (an arrow and the PVK symbol show the position of the voltammetric peak in Figure 3, data not shown) is a chemically irreversible process on these same voltammetric time scales. The peak potential for PVK oxidation is ca. 0.2 V more positive than that for the first oxidation of TPD, consistent with the larger ionization potential and HOMO energies for this material.<sup>9</sup> Previous electrochemical studies of substituted carbazoles show oxidation processes in this same potential range, with chemical stability dependent upon the substitution pattern of the carbazole.<sup>23</sup> The oxidation of *N*-ethyl carbazole is perhaps the best model of the oxidation of PVK and has demonstrated the following ECE reaction mechanism: formation of the cation radical, followed by coupling to form the 3,3'-dicarbazyl, and a subsequent loss of another electron to form a stable oxidation product. Such a coupling process would not be expected to be efficient in PVK oligomers or polymers and other chemical reaction pathways may exist for the PVK cation radical.

(22) (a) Flanagan, J. B.; Margel, S.; Bard, A. J.; Anson, F. C. *J. Am. Chem. Soc.* **1978**, *100*, 4248. (b) Saji, T.; Pasch, N. F.; Webber, S. E.; Bard, A. J. *J. Phys. Chem.* **1978**, *82*, 1101. (c) Pearce, P. J.; Bard, A. J. *J. Electroanal. Chem.* **1980**, *114*, 89.

(23) (a) Ambrose, J. F.; Nelson, R. F. *J. Electrochem. Soc.* **1968**, *115*, 1159. (b) Ambrose, J. F.; Carpenter, L. L.; Nelson, R. F. *J. Electrochem. Soc.* **1975**, *122*, 876.

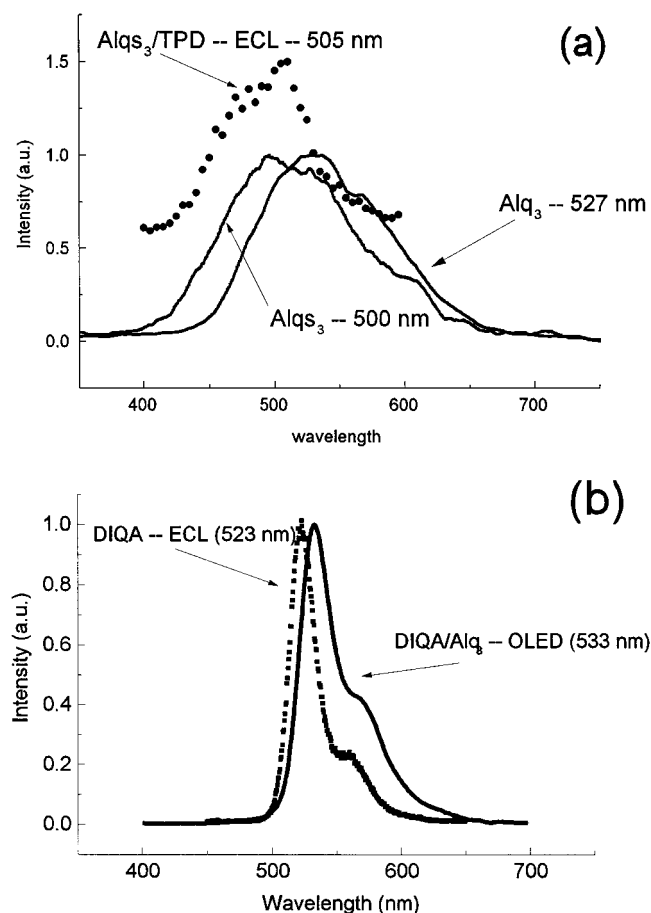


**Figure 4.** (a) ECL response for a typical double potential step experiment involving  $\text{Al}(\text{qs})_3^-/\text{TPD}^{+\bullet}$  (●●●) and the electroemissive spectral response for OLEDs (—) involving either  $\text{Alq}_3$  (vapor deposited as in the bilayer configuration in the left panel of Figure 1a or dissolved in PVK as in the right panel of Figure 1a) or  $\text{Al}(\text{qs})_3$ , dissolved in PVK as in the right panel of Figure 1a. (b) ECL response for a typical double potential step experiment involving the production of  $\text{DIQA}^{+\bullet}/\text{DIQA}^{-\bullet}$  (also  $\text{DIQA}^{-\bullet}/(\text{TPD}^{+\bullet}$  or  $\text{TPDF}_2^{+\bullet})$ ) and  $\text{DIQA}^{+\bullet}/(\text{Alq}_3^-$  or  $\text{Al}(\text{qs})_3^-)$  and the electroemissive spectral response from an  $\text{Alq}_3$ -based OLED, doped with ca. 1% w/w DIQA.

DIQA, **6**, showed two successive and reversible one-electron reduction processes and two successive oxidation processes, with good chemical stability for the first process and some instability for the second oxidation product. Cyclic voltammetry indicated that the first one-electron reduction and first one-electron oxidation products have half-lives exceeding tens of seconds in these dry degassed solvents. The first oxidation event occurred at potentials near those for the first oxidation of the  $\text{Alq}_3$  system, and ca. 0.3 V negative of the oxidation for  $\text{Al}(\text{qs})_3$ . The first reduction of DIQA occurred positive of the first reduction for the  $\text{Alq}_3$  system by ca. 0.46 V, and 0.14 V positive of the first reduction for  $\text{Al}(\text{qs})_3$  (Table 1). The solubility of QAD, **5**, in common electrochemical solvents is poor, and it was therefore difficult to obtain comparable electrochemical characterization of this molecule.

**ECL Reactions. Comparison with OLED Responses.** Figure 4a shows the emission spectra obtained from the ECL cross reaction of the cation radical of TPD with the anion radical of  $\text{Al}(\text{qs})_3$  (eq 5), initiated by multiple potential step experiments which created steady-state concentrations of both species in the diffusion layer adjacent to the working electrode on a time scale of hundreds of  $\mu\text{s}$ .<sup>13</sup> On this time scale, we expect the diffusion layer thickness where the ECL reactions occur to be ca. 700 nm. Similar emission spectra (shifted slightly in wavelength for

$\text{Al}(\text{qs})_3$  vs  $\text{Alq}_3$ ) are obtained for all of the cross reactions between the anion radicals of **1** (or **2**) and cation radicals of **3** (or **4**). Also shown in Figure 4a are the emission spectra from OLEDs using either **1** or **2** as lumophores, where both are dissolved in PVK matrixes<sup>10</sup> or where **1** is vapor-deposited on a TPD/ITO multilayer assembly.<sup>10</sup> These spectra are directly comparable with the emission spectra obtained by photoexcitation of comparable thickness films of these materials.<sup>14b</sup> The photoluminescence and OLED responses of **2** are slightly blue-shifted relative to the parent compound<sup>10,11</sup> as are the ECL responses measured in this study. The ECL cross reactions (eq 5) involving  $\text{Alq}_3$  or  $\text{Al}(\text{qs})_3$ , therefore, appear to produce a spectral response equivalent to that seen in the solid-state devices.

Figure 4b shows the emission spectra obtained from the direct anion/cation radical annihilation ECL processes (eq 6) of **6** (with a  $\lambda_{\text{max}}$  of 523 nm) and from an  $\text{Alq}_3$ -based OLED, doped with an optimal concentration (ca. 1.0 wt %) of this same quinacridone dye. Again, the emissive state produced by the ECL reaction appears to be the same as that produced in the OLED, shifted to slightly higher energy in solution form versus the condensed phase. These same emission spectra (within our experimental error) were also obtained for double ECL potential step processes involving cross reactions between  $\text{DIQA}^{-\bullet}$  and



$\text{TPD}^{+\bullet}$  (or  $\text{TPDF}_2^{+\bullet}$ ) and between  $\text{DIQA}^{+\bullet}$  and  $\text{Al}(\text{qs})_3^{-\bullet}$ .

The intensity of emission and therefore the signal-to-noise ratio for the ECL processes of DIQA are better (at equivalent concentrations) than for the aluminum quinolate direct reactions or the cross reactions with TPD (see below).

Figure 5a shows the type of ECL emission intensity vs time seen for a multiple potential step experiment at the microband electrode, in the presence of  $5 \times 10^{-4}$  M  $\text{Alq}_3$  and  $5 \times 10^{-4}$  M TPD. On both the negative potential step and the reverse step, the ECL intensity (integral of emission across the luminescence spectrum shown in Figure 4a) increased to a maximum ca. 80  $\mu\text{s}$  after the application of the potential step and then decayed back to zero counts prior to the application of the next potential step. The response was essentially equivalent for both negative-going and positive-going potential steps since the concentrations of both radical species had reached steady state in the diffusion layer by the time these data were recorded.<sup>13</sup>

The counts obtained from the average of several of these potential step experiments, compared with the counts obtained from the diphenylanthracene system, under comparable conditions,<sup>13d</sup> allowed for an estimation of the ECL efficiency of this cross reaction (Table 2). For the  $\text{Alq}_3/\text{TPD}$  system, with a difference in first reduction versus first oxidation potential ( $\Delta E = 2.65$  V), the computed efficiency was 0.09%. Switching to  $\text{TPDF}_2/\text{Alq}_3$ , with  $\Delta E = 2.75$  V, the ECL efficiency increased to 0.18%. Comparable behavior was seen with the  $\text{Al}(\text{qs})_3/\text{TPD}$  and  $\text{Al}(\text{qs})_3/\text{TPDF}_2$  systems. The  $\Delta E$  for the first process was 2.33 V, with a corresponding ECL efficiency of 0.03%, while the  $\Delta E$  for the second process was 2.43 V, with a corresponding ECL efficiency of 0.10%. In all of the cases, increasing the driving force for the cross reaction shown in eq 5 increased the corresponding ECL efficiency. Attempts to measure the ECL efficiency of the  $\text{Alq}_3$  system by itself (reactions involving  $\text{Alq}_3^{+\bullet}$  with  $\text{Alq}_3^{-\bullet}$ ) were difficult, owing to the irreversible adsorption accompanying oxidation of this

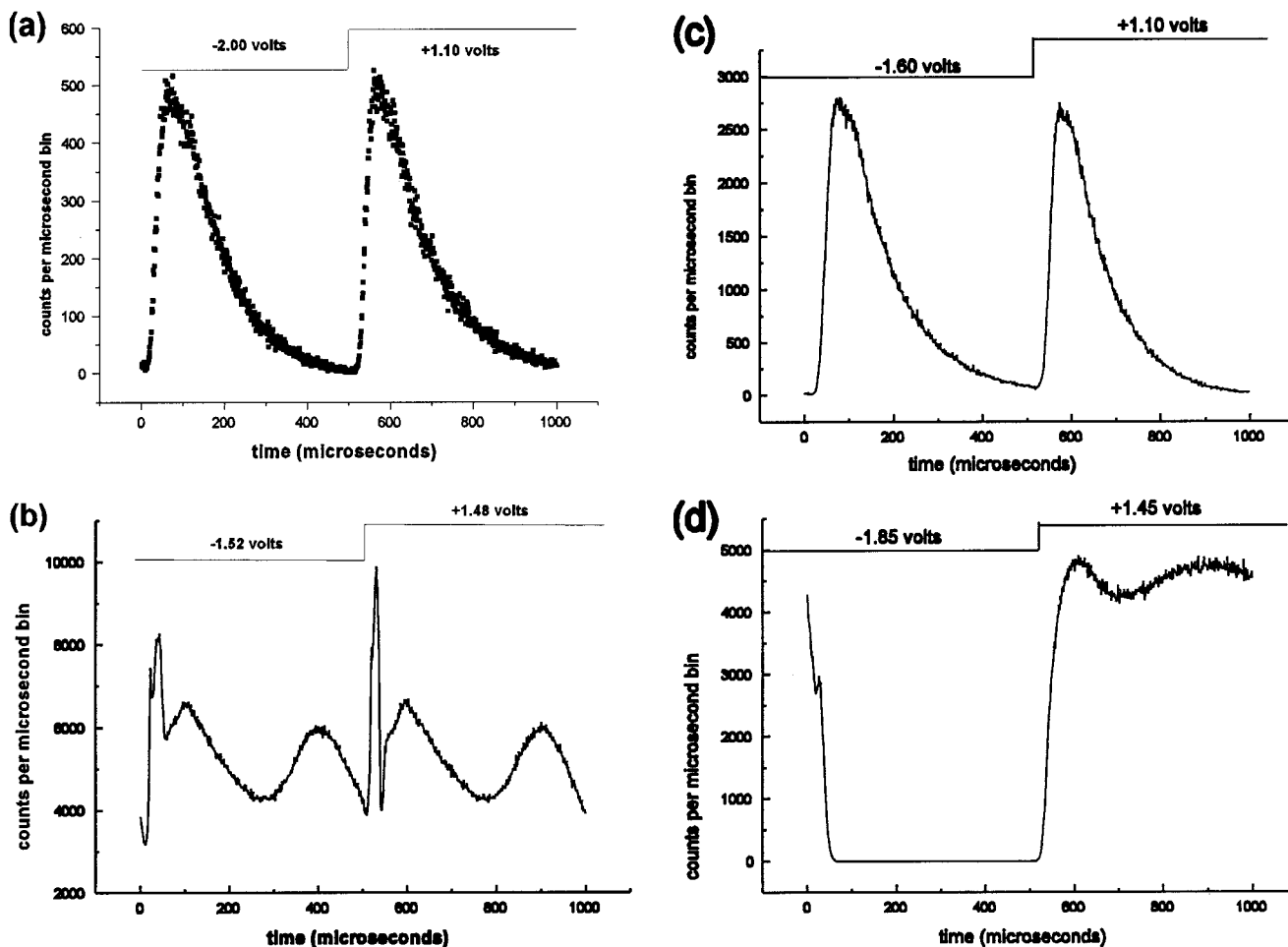


**Figure 5.** ECL emission intensity vs time for double potential step experiments involving: (a) solution  $5 \times 10^{-4}$  M in both  $\text{Alq}_3$  and TPD (forming  $\text{Alq}_3^{\cdot-}/\text{TPD}^{\cdot+}$ ), (b) solution of  $5 \times 10^{-4}$  M DIQA, (forming  $\text{DIQA}^{\cdot+}/\text{DIQA}^{\cdot-}$ ), (c) solution  $5 \times 10^{-4}$  M in both TPDF<sub>2</sub> and DIQA (forming  $\text{TPDF}_2^{\cdot+}/\text{DIQA}^{\cdot-}$ ), and (d) solution of  $5 \times 10^{-4}$  M  $\text{Al}(\text{qs})_3$  and  $1.7 \times 10^{-4}$  M DIQA (forming  $\text{Al}(\text{qs})_3^{\cdot-}/\text{DIQA}^{\cdot+}$ ). The results from panel (a) are the cumulative sum from 50 cycles, whereas the other panels represent the cumulative sum from 1000 cycles.

**Table 2.** ECL Efficiencies, Differences between First Oxidation and First Reduction Potentials, and Wavelengths of Maximum Emission, for Cross Reactions of  $\text{Alq}_3/\text{TPD}$  Couples and for Selected DIQA ECL Processes

anion radical forming species	cation radical forming species		
	TPD (3)	TPDF <sub>2</sub> (4)	DIQA (6)
$\text{Alq}_3$ (1)	$\Delta E^\circ = 2.65$ V $\phi = 0.09\%$ $\lambda_{\text{max}} = \text{ca. } 510$ nm	$\Delta E^\circ = 2.75$ V $\phi = 0.18\%$ $\lambda_{\text{max}} = \text{ca. } 510$ nm	
$\text{Al}(\text{qs})_3$ (2)	$\Delta E^\circ = 2.33$ V $\phi = 0.03\%$ $\lambda_{\text{max}} = \text{ca. } 510$ nm	$\Delta E^\circ = 2.43$ V $\phi = 0.10\%$ $\lambda_{\text{max}} = \text{ca. } 510$ nm	$\Delta E^\circ = 2.68$ V $\phi = 0.53\%$ $\lambda_{\text{max}} = 525$ nm
DIQA (6)		$\Delta E^\circ = 2.19$ V $\phi = 0.082\%$ $\lambda_{\text{max}} = 525$ nm	$\Delta E^\circ = 2.54$ V $\phi = 0.40\%$ $\lambda_{\text{max}} = 525$ nm

compound. Emitted light could be detected on the first few potential step cycles, but the counts were low and declined with successive potential steps.

Parts b, c, and d of Figures 5 show the ECL emission from experiments involving multiple potential steps in solutions of DIQA only ( $\text{DIQA}^{\cdot-}/\text{DIQA}^{\cdot+}$ , Figure 5b/eq 6),  $\text{DIQA}^{\cdot-}/\text{TPDF}_2^{\cdot+}$  (Figure 5c/eq 7), and  $\text{DIQA}^{\cdot+}/\text{Al}(\text{qs})_3^{\cdot-}$  (Figure 5d/eq 8). The emission/time profiles for the  $\text{DIQA}^{\cdot-}/\text{DIQA}^{\cdot+}$  experiment (Figure 5b) are complicated by an apparent adsorption process. The initial sharp rise in emission intensity with each potential step suggests an ECL process which is not diffusion controlled, followed by one or more diffusion-

controlled ECL processes involving solution soluble redox products. When the  $\text{TPDF}_2^{\cdot+}$  (or  $\text{TPD}^{\cdot+}$ )/ $\text{DIQA}^{\cdot-}$  reactions were examined (Figure 5c), the emission/time profiles returned to the expected form, suggesting that when  $\text{DIQA}^{\cdot+}$  was *not* formed, adsorption of redox species no longer influenced the ECL experiment. The data in Figure 5d was obtained with a 3:1 ratio of  $\text{Al}(\text{qs})_3/\text{DIQA}$  since the first reduction potentials of the two species were close to each other and we wished to determine whether the reaction of  $\text{Al}(\text{qs})_3^{\cdot-}$  with  $\text{DIQA}^{\cdot+}$  would produce the same type of ECL spectral response as the reaction of  $\text{TPD}^{\cdot+}$  with  $\text{DIQA}^{\cdot-}$ . As a result, ECL emission was only seen on  $1/2$  of the cycle. Despite the problems of adsorption of  $\text{DIQA}^{\cdot+}$  as seen in Figure 5b and d, all of the ECL experiments involving DIQA gave the spectral response shown in Figure 4b.

The ECL emission intensity arising from the radical annihilation reactions of  $\text{DIQA}^{\cdot-}/\text{DIQA}^{\cdot+}$  ( $\Delta E = 2.54$  V, ECL efficiency = 0.40%) was a factor of at least four greater than that seen for either the radical annihilation reactions of  $\text{Alq}_3$  alone or those of the cross reactions between  $\text{Alq}_3$  and the TPD compounds. The ECL behavior from the cross reactions  $\text{DIQA}^{\cdot-}/\text{TPD}$  or  $\text{DIQA}^{\cdot-}/\text{TPDF}_2$ , Figure 5c, was well behaved and had a lower efficiency (0.08%) than that for the  $\text{DIQA}^{\cdot-}/\text{DIQA}^{\cdot+}$  system, owing to the lower driving force for this reaction. The cross reactions  $\text{Al}(\text{qs})_3^{\cdot-}/\text{DIQA}^{\cdot+}$  (Figure 5d) showed the highest efficiencies seen in these experiments



(0.53%), again consistent with the higher driving force for this reaction ( $\Delta E = 2.68$  V).

## Conclusions

The initial work of Tang and VanSlyke and additional recent studies<sup>4</sup> have indicated that the emission from the aluminum quinolate OLEDs originates within 5 nm of the interface between the hole-transport layer and the lumophore layer. Because of the large negative reduction potential and poor electron-transporting properties of TPD and its derivatives, it is anticipated that electron-rich ( $\text{Alq}_3^-$ ) species will collect at the TPD/ $\text{Alq}_3$  interface and either undergo annihilation reactions with another cation radical species or chemically react with other radical species or impurities (e.g.,  $\text{O}_2$  and  $\text{H}_2\text{O}$ ). It has also been assumed that the electron-deficient species ( $\text{TPD}^{+\bullet}$ ) is capable of injecting holes (creating the  $\text{Alq}_3^{+\bullet}$  state) at the TPD/ $\text{Alq}_3$  interface, despite the energy barrier to this injection.

Our studies have shown that cross reactions between the cation radical state of the hole-transport agent and the anion radical state of the lumophore in  $\text{Alq}_3$ /TPD OLEDs can serve as a pathway to the production of the  $\text{Alq}_3^{*\text{s}}$  emissive state. Recent experiments with polymeric versions of TPD, polymeric methoxy-substituted TPD and the polymer version of the fluoro-substituted TPD, (**4**), in bilayer  $\text{Alq}_3$  OLEDs have shown that the overall efficiency of these devices scales with the first oxidation potential of the TPD derivative, as would be expected if the  $\text{Alq}_3^-/\text{TPD}^{+\bullet}$  cross reaction, whether it leads to singlet states directly or through a triplet pathway, is at least partially responsible for emissive state formation.<sup>24a</sup> Other recent experiments here have shown efficiency increases as the interfacial area (increased through texturing) of the  $\text{Alq}_3$ /TPD OLED increases, again consistent with formation of the  $\text{Alq}_3^{*\text{s}}$  state through a  $\text{TPD}^{+\bullet}/\text{Alq}_3^-$  cross reaction.<sup>24b</sup>

The cation radical state of TPD is also significantly more stable than the same state for  $\text{Alq}_3$ , and it would seem that it would be desirable to maximize the formation of emissive states through the pathways which prevent or slow the direct oxidation of  $\text{Alq}_3$ . At the same time, the anion radical state of DIQA, and by inference the parent quinacridone, is more stable than that state for  $\text{Alq}_3$ , suggesting that the formation of the DIQA emissive state, by trapping of the injected electron on this compound rather than on  $\text{Alq}_3$  would also increase the stability of the OLED.

In a single layer device, where the lumophore is dissolved directly into PVK (the cation radical state of which is a better oxidant than  $\text{TPD}^{+\bullet}$ ) or a triarylamine hole transporter has been dissolved into a polymer, there are no clear organic/organic' heterojunctions, and the ECL cross reactions discussed here are likely the dominant pathway for creation of the emissive state. Optimizing these reactions is critical to enhancing the efficiency of such devices.<sup>10</sup>

An issue yet to be resolved is whether the  $\text{Alq}_3$ /TPD ECL processes proceed by singlet versus triplet pathways to produce  $\text{Alq}_3^*$  and the extent to which such comparisons are relevant to the operation of the OLED. The  $\text{Alq}_3^-/\text{TPD}^{+\bullet}$  and  $\text{Alq}_3^-/\text{TPDF}_2^{+\bullet}$  solution reactions possess solution  $\Delta E^\circ$  values which exceed the energy of the  $\text{Alq}_3$  emissive state (2.4 eV), while the corresponding reactions involving  $\text{Al}(\text{qs})_3$  release energy at or just below this value. These energy differences are likely to be higher in the condensed phase, thereby favoring the singlet pathway. There is a possibility, however, that at least some of

the emissive-state formation proceeds by means of the lower probability triplet pathway, where the  $\text{Alq}_3^*$  singlet emissive state is formed not directly but rather through the annihilation of two proximate  $\text{Alq}_3^*$  triplet states formed from cross reactions where the energy released is at or below the singlet-state emissive energy.<sup>12,13</sup> There is precedence for this type of pathway in solution ECL cross reactions for molecules such as diphenylanthracene and other triaryl amines.<sup>13c</sup> The complete investigation of these possibilities, both in solution and in the condensed phase, is underway here for  $\text{Alq}_3$ /TPD and related systems.

The voltammetric responses for the redox processes of DIQA suggest that such modified quinacridones may function as charge traps for  $\text{Alq}_3^-$ ,  $\text{TPD}^{+\bullet}$ , and the cation radical state of the carbazole groups in PVK. While its absorption/luminescence spectra clearly suggest that Förster energy transfer from the  $\text{Alq}_3^{*\text{s}}$  emissive state to DIQA is likely, it is also apparent that this molecular species may act as a charge trap for some of the radical anion and radical cation species which may exist in the OLED and that direct or cross annihilation reactions involving  $\text{Alq}_3^-/\text{DIQA}^{+\bullet}$  and  $\text{DIQA}^-/\text{TPD}^{+\bullet}$  or  $\text{DIQA}^-/\text{PVK}^{+\bullet}$  may be responsible for some of the light emission from optimally doped versions of these OLEDs. The relative stability of the radical states of this molecule suggest that another attractive role for such dopants may be to stabilize the radical components created in the condensed phase. For DIQA to achieve all of these roles simultaneously, its optimum placement in the OLED would be at or quite near the HTL/LUM interface. Studies are underway to confirm this optimal location for DIQA and related OLED dopants.

We have also observed that PVK thin films incorporating only ca. 1–2 wt % of DIQA, with no  $\text{Alq}_3$  present, function as reasonable light-emitting devices.<sup>10</sup> Their output emission is limited by self-absorption of the emitted light, owing to the relatively small Stokes shift for DIQA (less than 20 nm in solution), and by the aggregation of these molecules at high concentrations in the condensed phase which leads to quenching of the luminescence.<sup>14d</sup> Studies now in progress seek to exploit the virtues of dopants for OLEDs which can act as both energy and charge acceptor species, as a way of enhancing light emission and possibly the chemical stability of these devices. Solution electrochemical studies of these molecular components will play an essential role in selecting components for these devices and in furthering our understanding of the radical ion reactions which occur there.

We anticipate that the electrochemical oxidation and reduction of solutions of components of the OLEDs will underestimate the energies necessary to carry out these redox processes in the condensed phase. Voltammetry of model compounds such as DPA in low dielectric constant solvents, with minimal supporting electrolyte (extrapolating to zero ionic strength), can be used to estimate how much larger the redox potentials of the OLED components will be in a condensed phase, low dielectric constant medium.<sup>13a</sup> Radical anion and cation states for these molecules are typically stabilized by ion pairing reactions with excess concentrations of supporting electrolyte in nonaqueous solvents, thereby decreasing the overall difference between the first reduction and first oxidation peak potentials at which those radical states are produced ( $\Delta E_p$ ), according to

$$\Delta E_p = \Delta E^{\circ'} + RT/nF \ln(K_{\text{AX}}K_{\text{MA}}) + 2RT/nF \ln c_{\text{M}^+} \quad (10)$$

where  $\Delta E^{\circ'}$  represents the maximum electrochemical potential difference between the formation of the radical anion and cation states,  $K_{\text{AX}}$  represents the ion pairing reaction of the cation

(24) (a) Jabbour, G. E.; Belman, E.; Marder, S. R.; Grubbs, R.; Kippelen, B.; Peyghambarian, N. *Chem. Mater.*, submitted. (b) Jabbour, G. E., personal communication.

radical state with the supporting electrolyte anion,  $K_{MA}$  represents the ion pairing reaction of the anion state with the supporting electrolyte cation, and  $c_{M+}$  is the concentration of the supporting electrolyte.<sup>25</sup> We can assume that the thin film environment will act as a low dielectric constant solvent for the radical ions created at the injecting electrodes, with no supporting electrolyte ions to help screen or ion-pair the created charges. We cannot, however, anticipate the effect of having high concentrations of both radical molecular components in a thin film space of no more than 100–200 nm at the current densities typically used in these OLEDs (0.1 to 1.0 A/cm<sup>2</sup>), which may lead to some stabilization due to ion pairing effects prior to annihilation reactions.

The difference between frontier orbital energies in the condensed phase ( $\Delta E$ ) can be estimated from measured differences in the onset for photoemission in the UPS experiment and the onset for inverse photoemission (IPES), if available,<sup>21</sup> or from differences in gas-phase ionization potential and electron affinity, modified by the stabilization energies for the cation and anion forms of the molecule in the condensed phase and the stabilization of the ground-state molecule in going from the gas phase to the condensed phase.<sup>26</sup> For weakly interacting molecular solids, it is anticipated that  $\Delta E$  in the condensed phase will be comparable to that observed in solution, with differences

arising due to differences in energies of stabilization of the oxidized and reduced forms of these molecules in solution versus the solid thin film. As recently shown for crystalline films of perylene dyes and C<sub>60</sub>, it is necessary to directly measure the electron affinity of the molecular solid, in the condensed phase, to ascertain the difference in  $\Delta E$  estimated from UPS/optical studies, as shown here, and that  $\Delta E$  which actually pertains to charge injection into the solid material.<sup>21</sup> Nevertheless, the electrochemical measurements available now give us the ability to estimate the lower limit to the values for  $\Delta E$  in the condensed phase and show that both the direct and ECL cross reactions are likely to be energy sufficient in the OLED. Work in progress seeks to exploit these principles in the optimization of polymer-based versions of these and related OLEDs.

**Acknowledgment.** Support for this work was provided by the Center for Advanced Multifunctional Polymers and Molecular Assemblies (CAMP), a DOD/ONR/MURI program, by the National Science Foundation (NRA and MW), and by the Materials Characterization Program, State of Arizona. We also gratefully acknowledge very helpful recent discussions with Professor Jean-Pol Dodelet, INRS-Quebec.

JA980707+

(25) (a) Peover, M. E.; Davies, J. D. *J. Electroanal. Chem.* **1963**, *6*, 46. (b) Peover, M. E. In *Electroanalytical Chemistry, A Series of Advances*; Bard, A. J., Eds.; Marcel Dekker: New York, Vol. 2, 1967; p 40.

(26) Wright, J. D. *Molecular Crystals*, 2nd ed.; Cambridge University Press: Redwood Books, Trowbridge, Wiltshire, England, 1995; pp 144–169 and references therein.